Gravitational Wave Study in Leptophobic Models

Exploring the Dynamics and Detection Prospects

TARAMATI

PhD Supervisor: Dr. Sudhanwa Patra
Collaboration with Lekhika Malhotra, Zafri A. Borboruah

PPC-2024 IIT Hyderabad

17[th] International Conference on Interconnections between Particle Physics and Cosmology

PPC 2024

14 -18 October 2024, Hyderabad, India

October 16, 2024

Outline

1. Motivations
2. Gravitational wave
3. Model framework
4. Phase transition and Effective potential
5. Phase transition plot with different parameter space
6. Gravitational wave plots with different parameter space
7. Discussion on direct-detection Bounds and relic density bounds
8. Conclusion

Motivations

- Study about gravitational wave signals in leptophobic model.
- Probing the Dark matter through the gravitational wave signals.
- Develope the connection between the dark matter and gravitational wave.

Taramati, R.Sahu, U.Patel, S.Patra-:2408.12424.

Gravitational wave and dark matter

Gravitational waves are ripples in the fabric of spacetime caused by certain movements of mass, such as the acceleration of massive objects, particularly those involving strong gravity. First predicted by Albert Einstein in 1916.

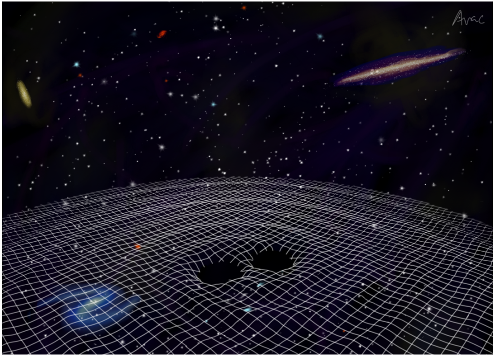

Figure 1: www.quantumuniverse.nl/app/uploads/2023/11

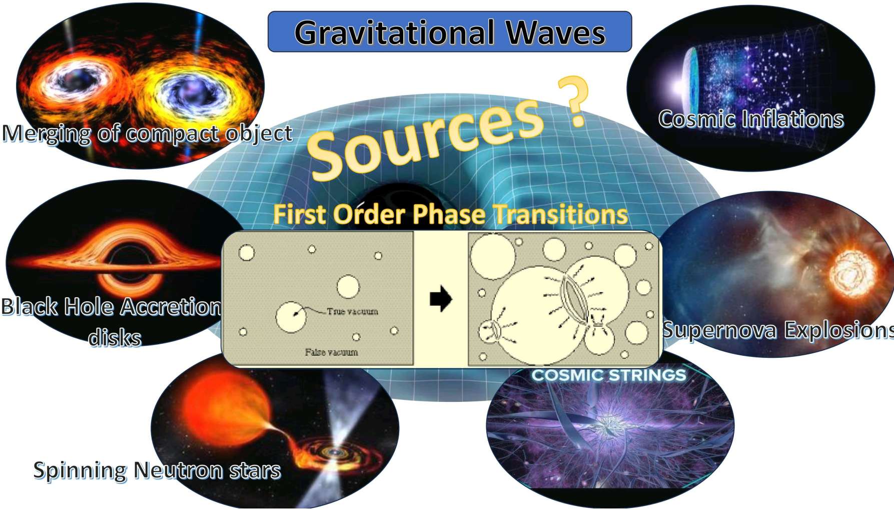
Gravitational Waves
Sources ?
Merging of compact object
Cosmic Inflations
First Order Phase Transitions
True vacuum
False vacuum
Black Hole Accretion disks
Supernova Explosions
COSMIC STRINGS
Spinning Neutron stars

GW Experiments

KARGA, Hida, Japan

NANOGrav, United State, Canada

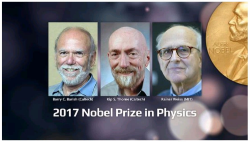

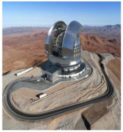

Einstein Telescope, Europe

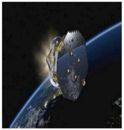

LISA Space based Observatory

VIRGO, Italy

Pulsar Timing Arrays,

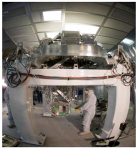

LIGO, US ,Washington

How to Probe It ?

Leptophobic Model

$$\Updownarrow$$

$$SU(3)_C \otimes SU(2)_L \otimes U(1)_Y \otimes U(1)_B$$

Taramati, R.Sahu, U.Patel, S.Patra-:2408.12424.

Model Framework

$$\mathcal{A}[SU(3)_C^2 \times U(1)_B] = 0$$

$$\mathcal{A}[SU(2)_L^2 \times U(1)_B] = \frac{3}{2}$$

$$\mathcal{A}[U(1)_Y^2 \times U(1)_B] = -\frac{3}{2}$$

$$\mathcal{A}[U(1)_Y \times U(1)_B^2] = 0$$

$$\mathcal{A}[U(1)_Y^2 \times U(1)_B] = 0$$

$$\mathcal{A}[U(1)_Y \times U(1)_B^2] = 0$$

$$B_1 - B_2 = -3$$

Two anomalies arises, for cancellation we are adding the 6 fermionic particles.

Gauge fields	$SU(2)_L$ $\vec{W}_\mu$	$U(1)_Y$ B_μ	$U(1)_B$ Z'_μ
$\Psi_L = \begin{pmatrix} \Psi^+_{1L} \\ \Psi^0_{1L} \end{pmatrix}$	**2**	1/2	B_1
$\Psi_R = \begin{pmatrix} \Psi^+_{2R} \\ \Psi^0_{2R} \end{pmatrix}$	**2**	1/2	B_2
$\xi_L = \xi_L^+$	**1**	1	B_2
$\xi_R = \xi_R^+$	**1**	1	B_1
$\chi_L = \chi_L^0$	**1**	0	B_2
$\chi_R = \chi_R^0$	**1**	0	B_1
H	**2**	1/2	0
S	**1**	0	$B_1 - B_2$

$B_1 = -1$ and $B_2 = 2$

Model Framework

The complete Lagrangian for the gauge theory of baryons is given by

$$
\begin{aligned}
\mathcal{L} \;=\;& \mathcal{L}_{\mathrm{SM}} - \frac{g_B}{3}\left[\overline{q_L}\gamma_\mu Z_B^\mu q_L + \overline{u_R}\gamma_\mu Z_B^\mu u_R + \overline{d_R}\gamma_\mu Z_B^\mu d_R\right] \\
& + \overline{\Psi_L} i \not{D} \Psi_L + \overline{\Psi_R} i \not{D} \Psi_R + \overline{\chi_L} i \not{D} \chi_L + \overline{\chi_R} i \not{D} \chi_R + \overline{\xi_L} i \not{D} \xi_L + \overline{\xi_R} i \not{D} \xi_R \\
& - \left[h_1 \overline{\Psi_L} \tilde{H} \xi_R + h_2 \overline{\Psi_R} \tilde{H} \xi_L + h_3 \overline{\Psi_L} H \chi_R + h_4 \overline{\Psi_R} H \chi_L\right] \\
& - \left[\lambda_\Psi \overline{\Psi_L} S_B \Psi_R + \lambda_\xi \overline{\xi_L} S_B \xi_R + \lambda_\chi \overline{\chi_L} S_B \chi_R\right] + h.c. \\
& + (D_\mu S_B)^\dagger (D^\mu S_B) - V(H, S_B) \qquad (1)
\end{aligned}
$$

The Yukawa potential term is written by

$$
\begin{aligned}
\mathcal{L}_{NF}^{B} \;=\;& \overline{\begin{pmatrix} \Psi_{1L}^{+} & \xi_L^{+} \end{pmatrix}} \begin{pmatrix} M_\Psi & M_1 \\ M_2 & M_\xi \end{pmatrix} \begin{pmatrix} \Psi_{2R}^{+} \\ \xi_R^{+} \end{pmatrix} \\
& + \overline{\begin{pmatrix} \chi_L^{0} & \Psi_{1L}^{0} \end{pmatrix}} \begin{pmatrix} M_\chi & M_4 \\ M_3 & M_\Psi \end{pmatrix} \begin{pmatrix} \chi_R^{0} \\ \Psi_{2R}^{0} \end{pmatrix} + h.c., \qquad (2)
\end{aligned}
$$

- Whose mass term are listed below,
$M_\Psi = \frac{\lambda_\Psi v_B}{\sqrt{2}}, \quad M_\xi = \frac{\lambda_\xi v_B}{\sqrt{2}}, \quad M_1 = \frac{h_1 v}{\sqrt{2}}, \quad M_2 = \frac{h_2 v}{\sqrt{2}},$
$M_3 = \frac{h_3 v}{\sqrt{2}}, \quad M_4 = \frac{h_4 v}{\sqrt{2}}$
- The unphysical flavor basis $\begin{pmatrix} \chi_L^0 & \Psi_L^0 \end{pmatrix}^T$ is related to physical mass basis $\begin{pmatrix} \Psi_{1L} & \Psi_{2L} \end{pmatrix}^T$ basis as,
$\begin{pmatrix} \Psi_{1L} \\ \Psi_{2L} \end{pmatrix} = \mathcal{V} \begin{pmatrix} \chi_L^0 \\ \Psi_L^0 \end{pmatrix}$ Similarly, $\begin{pmatrix} \Psi_{1R} \\ \Psi_{2R} \end{pmatrix} = \mathcal{V} \begin{pmatrix} \chi_R^0 \\ \Psi_R^0 \end{pmatrix}$,
$\mathcal{V} = \begin{pmatrix} \cos\theta_{L/R} & \sin\theta_{L/R} \\ -\sin\theta_{L/R} & \cos\theta_{L/R} \end{pmatrix}$
- Here, $\Psi_1 = \Psi_{1L} + \Psi_{1R}$, $\Psi_2 = \Psi_{2L} + \Psi_{2R}$, the lighter one among them is a viable DM candidate.

Continued....

- Now, combining the chiral states of χ^0 and Ψ^0, is reduced to,

$$\begin{aligned} \Psi_1 &= \cos\theta_{LR}(\chi^0) + \sin\theta_{LR}(\Psi^0) \\ \Psi_2 &= -\sin\theta_{LR}(\chi^0) + \cos\theta_{LR}(\Psi^0) \end{aligned} \tag{3}$$

- Where the mixing angle $\tan 2\theta_{DM} = \frac{M_4+M_3}{M_\Psi - M_\chi}$ Here, $m \simeq M_4 + M_3$.
- The mass eigenvalues of the physical states Ψ_1 and Ψ_2 are respectively given by,(for small $\sin\theta_{DM/LR}$ $(\sin\theta_{DM} \to 0)$ limit, m_{Ψ_1} and m_{Ψ_2})

$$\begin{aligned} m_{\Psi_1} &\simeq M_\chi + m\sin 2\theta_{DM} \equiv M_\chi - \frac{(2m^2)}{(M_\Psi - M_\chi)}, \\ m_{\Psi_2} &\simeq M_\Psi - m\sin 2\theta_{DM} \equiv M_\Psi + \frac{2m^2}{(M_\Psi - M\chi)}. \end{aligned} \tag{4}$$

- In the limit $m \ll m_\chi < m_\Psi$, we can get $m_{\Psi_1} < m_{\Psi_2}$. Thus, the lightest Dirac fermion Ψ_1 is the stable dark matter(DM) candidate.

$$V_{\rm eff}(\varphi_S, T) = V_0(\varphi_S) + V_{\rm CW}(\varphi_S) + V_{\rm CT}(\varphi_S) + V_{\rm T}(\varphi_S, T) + V_D(\varphi_S, T)$$

Here:

- $V_0(\varphi_S) = -\frac{\mu_S^2}{2}\varphi_S^2 + \frac{\lambda_S}{4}\varphi_S^4.$
- $V_{\rm CW}(\varphi_S) = \frac{1}{64\pi^2}\sum_i n_i\,(-1)^{2s_i}\,M_i^4(\varphi_S)\left(\log\left[\frac{M_i^2(\varphi_S)}{\Lambda^2}\right] - C_i\right).$
- $V_{\rm CT}(\varphi_S) = -\frac{\delta\mu_S^2}{2}\varphi_S^2 + \frac{\delta\lambda_S}{4}\varphi_S^4,$

  $\left.\frac{\partial^2 V_{CT}(\varphi_S)}{\partial\varphi_S^2}\right|_{\varphi_S = v_B} = -\left.\frac{\partial^2 V_{CW}(\varphi_S)}{\partial\varphi_S^2}\right|_{\varphi_S = v_B},$

  $\left.\frac{\partial V_{CT}(\varphi_S)}{\partial\varphi_S}\right|_{\varphi_S = v_B} = -\left.\frac{\partial V_{CW}(\varphi_S)}{\partial\varphi_S}\right|_{\varphi_S = v_B}.$

Continue...

- $V_{\mathrm{T}}(\varphi_S, T) = \frac{T^4}{2\pi^2} \sum_i n_i J_i \left(\frac{m_i^2(\varphi_S)}{T^2}\right)$,

  Here, $J_{B,F}(y^2) = \int_0^\infty \mathrm{d}x \; x^2 \log\left(1 \mp e^{-\sqrt{x^2+y^2}}\right)$.
- $V_D(\varphi_S, T) = -\frac{T}{12\pi} \sum_i n_i \left[\left(m_i^2(\varphi_S) + \Pi_i(T)\right)^{3/2} \left(m_i^2(\varphi_S)\right)^{3/2}\right]$

- **Parameters**:-
- Coupling constant $\lambda_\Psi, \lambda_\chi, \lambda_\xi, \lambda_S, \lambda_{HS}$.
- Degree of freedom (g) and $(g*)$.
- Critical temperature T_c and nucleation temperature T_n.
- α and β parameters.

Phase transition plots with differents parameters space

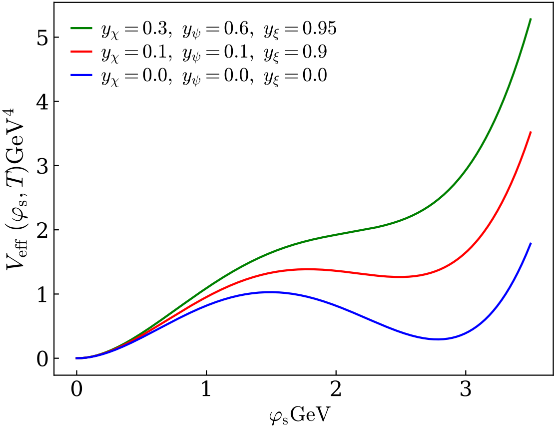

Figure 2: Effective plot at a temperature T=2.27TeV, with quartic coupling $\lambda_S = 0.0035$, $v_B = 5\mathrm{TeV}$ and $g_B = 0.67$. differents colors lines represents differents values of the Yukawa couplings y_χ, y_Ψ, y_ξ.

Understanding of GW through FOPT

- Step1 Calculate the nucleation rate:

$$\Gamma(T) \approx T^4 \left(\frac{S_3}{2\pi T}\right)^{3/2} e^{-\frac{S_3}{T}}$$

- Step2 Solve the differential equation to get the bubble profile:

$$\frac{d^2\varphi_S}{dx^2} + \frac{2}{x}\frac{d\varphi_S}{dx} = \frac{dV_{\rm eff}(\varphi_S, T)}{d\varphi_S}$$

- Step3 Find action:

$$S_3 = \int_0^\infty \mathrm{d}x \mathrm{d}x^2 \left[\frac{1}{2}\left(\frac{\mathrm{d}\varphi_S(x)}{\mathrm{d}x}\right)^2 + V(\varphi_S, T)\right].$$

- Step4 α and β parameters:

$$\alpha = \frac{\rho_{\rm vac}}{\rho_{\rm rad}} = \frac{1}{\rho_{\rm rad}}\left[\frac{T}{4}\frac{\mathrm{d}\Delta V}{\mathrm{d}T} - \Delta V\right]_{T_n}$$

$$\beta = \left(\mathcal{H} T \frac{\mathrm{d}(S_3/T)}{\mathrm{d}T}\right)_{T_n}$$

Phase transition plots with differents parameters space

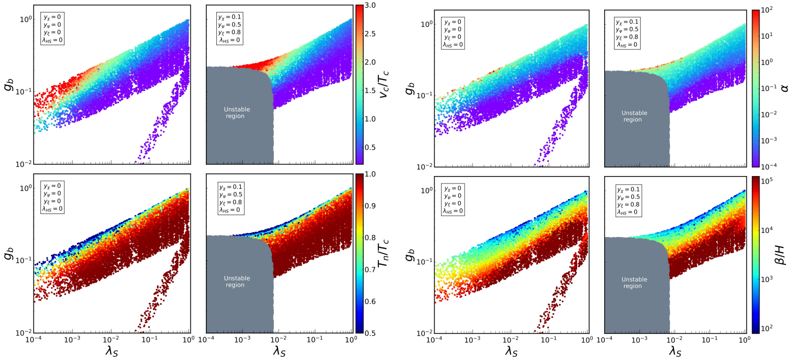

Figure 3: Plot of v_c/T_c**(left Top)** and T_n/T_c **(left Bottom)** and α **(right Top)** and β/H **(right Bottom)** in parameter space involving quartic coupling λ_S and gauge coupling g_B assuming portal coupling $\lambda_{HS} = 0$. Each point indicates an FOPT.

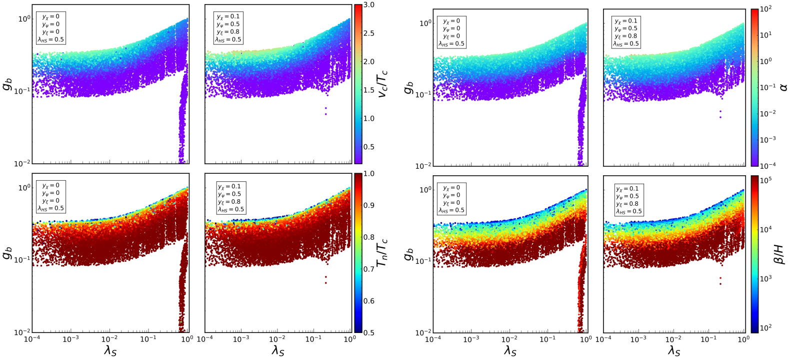

Figure 4: Same as Fig. 2 but for $\lambda_{HS} = 0.5$. The potential is stable even in the **(Right)** panel due to enhanced contribution of the scalar sector to the effective potential..

$$v_B \in [10^2, 10^6]\ \mathrm{GeV},\ \lambda_S \in [10^{-4}, 1],\ g_B \in [10^{-4}, 1],\ \lambda_{HS} \in 0 \text{ or } 0.5,\ y_{\chi,\psi,\xi} \in [0, 1]$$

Sources of gravitational wave

$$\Omega_{\rm GW} h^2 \simeq \Omega_{\rm sw} h^2 + \Omega_{\rm turb} h^2 + \Omega_{\rm coll} h^2.$$

- Collision of bubble(runway) walls and (where relevant) shocks in the plasma.
- Sound waves(non-runway) in the plasma after the bubbles have collided but before expansion has dissipated the kinetic energy.
- Magneto-Hydrodynamic (MHD) turbulance(runway in vaccum) in the plasma forming after the bubbles have collided.

$$\Omega_{\rm sw}(f)h^2 = 2.65 \times 10^{-6} \left(\frac{H_*}{\beta}\right) \left(\frac{\kappa_{sw}\,\alpha}{1+\alpha}\right)^2 \left(\frac{100}{g_*}\right)^{\frac{1}{3}} v_w \left(\frac{f}{f_{\rm sw}}\right)^3 \left(\frac{7}{4+3\,(f/f_{\rm sw})^2}\right)^{7/2} \Upsilon$$

$$\text{here, } f_{\rm sw} = \frac{1.9\times10^{-5}}{v_w} \left(\frac{\beta}{H_*}\right) \left(\frac{T_*}{100\mathrm{GeV}}\right) \left(\frac{g_*}{100}\right)^{\frac{1}{6}} \mathrm{Hz}$$

$$\Omega_{\rm turb} h^2 = 3.35 \times 10^{-4} \left(\frac{H_*}{\beta}\right) \left(\frac{\kappa_{\rm turb}\ \alpha}{1+\alpha}\right)^{\frac{3}{2}} \left(\frac{100}{g_*}\right)^{1/3} v_w \frac{(f/f_{\rm turb}\ )^3}{[1+(f/f_{\rm turb}\ )]^{\frac{11}{3}}\ (1+8\pi f/h_*)}$$

where $\kappa_{\rm turb} = 0.05\kappa_{\rm turb}$ and, $h_* = 16.5 \cdot 10^{-6} \left(\frac{T_n}{100\mathrm{GeV}}\right) \left(\frac{g_*}{100}\right)^{1/6}$ Hz The peak frequency is given by:

$$f_{\rm turb} = \frac{2.7\times10^{-5}}{v_w} \left(\frac{\beta}{H_*}\right) \left(\frac{T_*}{100\mathrm{GeV}}\right) \left(\frac{g_*}{100}\right)^{\frac{1}{6}} \mathrm{Hz}$$

$$h^2\Omega_{\rm coll}(f) = \underbrace{1.67\times10^{-5}\left(\frac{g_*}{100}\right)^{-\frac{1}{3}}}_{\color{red}{Redshift}} \underbrace{\left(\frac{\kappa_{\rm coll}\alpha}{1+\alpha}\right)^2\left(\frac{\beta}{H_*}\right)^{-2}\Delta(f_{\rm coll},v_w)}_{\color{green}{Scaling}}\ \underbrace{S_{\rm coll}(f,v_w)}_{\color{blue}{Shape}},$$

$$f_{\rm coll} = \underbrace{1.65\times10^{-5}\,\mathrm{Hz}\left(\frac{g_*}{100}\right)^{\frac{1}{6}}\left(\frac{T_*}{100\,\mathrm{GeV}}\right)\left(\frac{f_*}{\beta}\right)\left(\frac{\beta}{H_*}\right)}_{\color{red}{Redshift}},$$

Gravitational wave plots

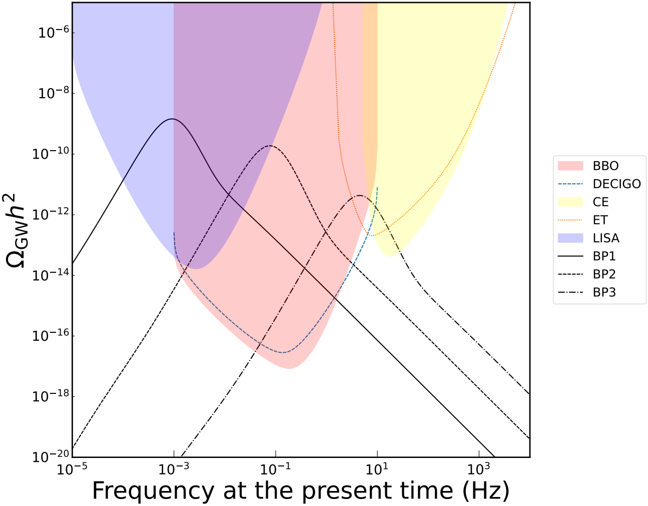

Figure 5: Spectrum plots with benchmark points.

Benchmark points for the spectrum plot

	BP1	BP2	BP3
v_B(GeV)	6429.38	55399.27	928114.36
λ_S	0.0057	0.0064	0.0015
g_B	0.247	0.191	0.162
λ_{HS}	0	0	0
y_χ	0.055	0.0093	0.0025
y_ψ	0.007	0.143	0.048
y_ξ	0.012	0.004	0.0020
$T_c/$GeV	2742.41	24631.03	284870.01
$T_n/$GeV	236.99	4062.15	40845.63
v_c/T_c	2.344	2.248	3.257
α	212.647	13.468	30.181
α_∞	0.0025	0.0028	0.0013
β/H_*	19.623	96.533	559.718

Table 1: Benchmark points for FOPT

Connection between GW and Dark matter

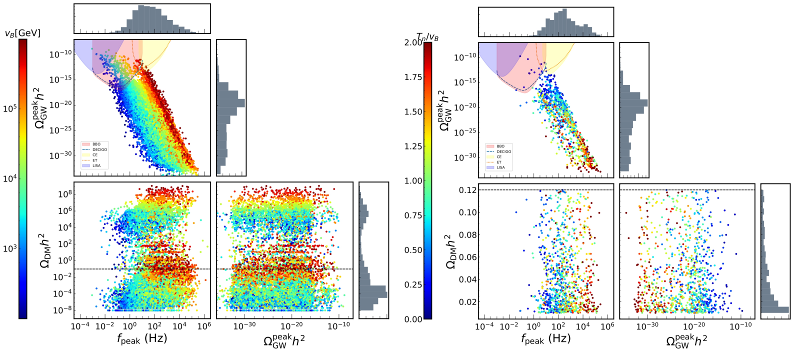

Figure 6: Distribution plots with $\lambda_{HS} = 0$.

With non zero mixing coupling...

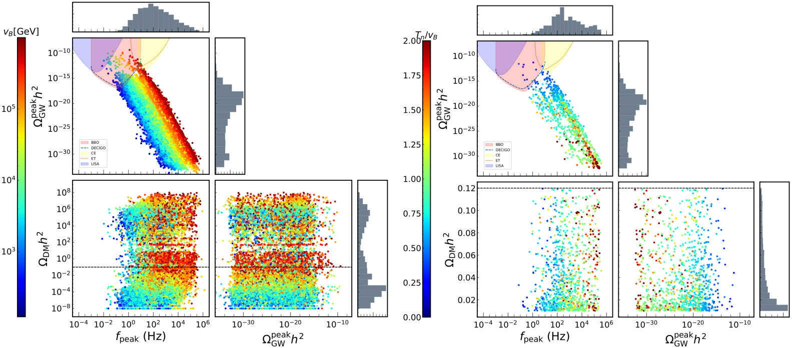

Figure 7: Distribution plots with $\lambda_{HS} = 0.5$

Benchmark point...

Parameters	BP1	BP2	BP3	BP4	BP5
$M_{\rm DM}$	78.77	52.33	101.74	72.81	25.73
SIDD	3.38×10^{-49}	1.8×10^{-49}	1.66×10^{-49}	1×10^{-51}	1.22×10^{-48}
$\Omega_{\rm DM}h^2$	0.112	0.105	0.108	0.128	0.122
λ_S	5.36×10^{-3}	6.03×10^{-3}	2.76×10^{-3}	1.23×10^{-3}	3.57×10^{-3}
v_b	31423.70	36647.79	37572.64	144076.64	22505.61
g_B	1.56×10^{-1}	1.08×10^{-1}	6.76×10^{-2}	1.30×10^{-1}	1.30×10^{-1}
y_χ	3.54×10^{-3}	2.02×10^{-3}	3.82×10^{-3}	7.14×10^{-4}	1.61×10^{-3}
y_Ψ	3.88×10^{-3}	7.03×10^{-3}	7.78×10^{-3}	7.89×10^{-4}	1.84×10^{-3}
y_ξ	2.52×10^{-1}	2.18×10^{-3}	3.97×10^{-3}	6.55×10^{-2}	2.38×10^{-2}
T_c	19740.7	32064.9	37703.42	53067.35	43407.63
T_n	18430.77	31594.60	37613.76	36013.61	12248.47
v_c/T_c	1.208	5.61×10^{-1}	2.39×10^{-1}	2.66	1.3523
α	2.58×10^{-3}	2.83×10^{-4}	1.769×10^{-5}	2.45×10^{-2}	2.61×10^{-3}
β/H	4635.24	16655.11	99657.28	2128.67	4048.89
α_{inf}	1.44×10^{-3}	6.864×10^{-4}	2.42×10^{-4}	8.66×10^{-4}	8.904×10^{-4}

Figure 8: Benchmark points for $\lambda_{HS} = 0$ which are allowed from SIDD cross section and relic density. We have implemented the model on SARAH, micrOmegas and SPheno for obtaining the SIDD cross section and relic density..

Continue...

Parameters	BP1	BP2	BP3	BP4	BP5	BP6
$M_{\rm DM}$	85.68	39.73	205.47	2.20	424.51	86.94
SIDD	1×10^{-51}	3.2×10^{-47}	1.18×10^{-47}	4.14×10^{-48}	1.8×10^{-50}	8.72×10^{-48}
$\Omega_{\rm DM}h^2$	0.112	0.121	0.105	0.112	0.119	0.118
λ_S	4.33×10^{-3}	7.35×10^{-1}	7.12×10^{-3}	4.62×10^{-1}	9.31×10^{-4}	3.75×10^{-3}
v_b	188560.73	10015.8	20677.7	14145.05	344811.6	19041.50
g_B	1.61×10^{-1}	3.70×10^{-2}	1.69×10^{-1}	6.17×10^{-1}	3.13×10^{-1}	2.07×10^{-1}
y_χ	6.42×10^{-4}	5.61×10^{-3}	1.40×10^{-2}	2.20×10^{-4}	1.74×10^{-3}	6.45×10^{-3}
y_Ψ	2.39×10^{-3}	6.67×10^{-3}	2.32×10^{-1}	2.53×10^{-1}	1.77×10^{-3}	5.32×10^{-2}
y_χ	6.71×10^{-4}	1.09×10^{-1}	1.41×10^{-2}	2.59×10^{-4}	5.08×10^{-3}	6.75×10^{-3}
T_c	18639.31	36501.11	19821.57	19796.57	211559.4	15098.36
T_n	182389.48	36486.04	19790.8	18719.6	183760.6	14854.67
v_c/T_c	2.40×10^{-1}	7.2×10^{-2}	2.56×10^{-1}	6.52×10^{-1}	1.38	6.63×10^{-1}
α	2.15×10^{-4}	2.47×10^{-5}	2.72×10^{-4}	9.38×10^{-3}	1.71×10^{-2}	2.18×10^{-3}
β/H	163474.3	581964.2	143832.2	4231.47	1644.71	14065.30
α_{inf}	1.12×10^{-3}	1.56×10^{-2}	1.64×10^{-3}	2.83×10^{-2}	3.9×10^{-3}	2.15×10^{-3}
λ_H	14.54	2.14×10^{-1}	8.92	2.64×10^{-1}	67.21	16.86

Figure 9: Same as fig 8 $\lambda_{HS} = 0.5$ which are allowed from SIDD cross section and relic density.

Conclusion....

- SFOPT requires small quartic coupling $\lambda_S \lesssim 0.01$ and relatively large gauge coupling $g_B > 0.01$. The strength of the phase transition is usually stronger near the supercooled limit in the parameter space. However a non-zero portal coupling reduces the overall strength and increases the stability of the effective potential by enhancing the scalar contribution to it.
- On the other hand large Yukawa couplings $y_{\chi,\psi,\xi}$ of the exotic fermions contribute negatively to the effective potential rendering it unstable in the small λ_H and g_B limit (see Fig. 3-4).
- The peak of the GW spectrum depends on the scale of $U(1)_B$ breaking v_B. For the 3 benchmark points given in Table 1 with $v_B \sim \mathcal{O}(1), \mathcal{O}(10)$ and $\mathcal{O}(100)$ TeV, the resultant peaks of the GW spectra with peak frequencies $\mathcal{O}(10^{-3}), \mathcal{O}(0.1)$ and $\mathcal{O}(10)$ Hz lie within the sensitivity of LISA, BBO and ET respectively (5).

Conclusion....

- The random parameter scan shows our model can generate GW signals with peak frequency ranging from $\sim 10^{-3}$ to 10^{6} Hz and peak amplitude ranging from $\sim 10^{-35}$ to 10^{-10} for the $v_B \in (10^2, 10^6)$ GeV. Only a fraction of these will be detected in LISA, BBO, DECIGO, CE and ET.
- Also many of these parameter points overcloses the Universe by producing excessive relic density (Fig. 6 and 7).
- However, still a small fraction satisfies the correct relic density condition along with being observable in the said experiments in the future (Fig. 6 and 7)

References:-

- T. Bringmann, T. E. Gonzalo, F. Kahlhoefer, J. Matuszak, and C. Tasillo, "Hunting WIMPs with LISA: Correlating dark matter and gravitational wave signals," arXiv:2311.06346.
- S. R. Coleman and E. J. Weinberg, "Radiative Corrections as the Origin of Spontaneous Symmetry Breaking," Phys. Rev. D 7 (1973) 1888–1910.
- P. Basler, M. Krause, M. Muhlleitner, J. Wittbrodt, and A. Wlotzka, "Strong First Order Electroweak Phase Transition in the CP-Conserving 2HDM Revisited," JHEP 02 (2017) 121, arXiv:1612.04086.
- M. Quiros, "Finite temperature field theory and phase transitions," in ICTP Summer School in High-Energy Physics and Cosmology, pp. 187–259. 1, 1999. arXiv:hep-ph/9901312.

Thanks :)